Effects of ramp vibrational states on flexural intrinsic vibrations in Besocke-style scanners*

Zhang Hui(张 辉)†, Jiang Guo-Zhu(蒋国珠), Liu Zhao-Qun(刘朝群), Zhang Shu-Yi(张淑仪), and Fan Li(范 理)

Laboratory of Modern Acoustics, Institute of Acoustics, Nanjing University, Nanjing 210093, *China*

(Received 6 September 2012; revised manuscript received 18 December 2012)

For both the vibrating and steady supporting surfaces of a scanning disk in a Besocke-style piezoelectric scanner, a theoretical model is given by considering the nonlinear lateral friction at the micro-contact interface between the positioning legs and the supporting surface. Numerical simulations demonstrate that unexpected flexural vibrations can arise from a vibrating ramp, and their frequencies are lower than the eigenfrequencies of the scanner in the linearly elastic regime. The vibrations essentially depend on 1) the vibrational states of the supporting ramp and the steel ball tips on the three piezoelectric positioning legs, and 2) the tribological characteristics of the contacts between the tips and the ramp. The results give an insight into the intrinsic vibrations of the scanners, and are applicable in designing and optimizing piezoelectric scanning systems.

Keywords: Besocke-style scanner, stick-slip behavior, flexural vibration, Timoshenko beam theory

PACS: 81.40.Pq, 46.55.+d, 07.79.Sp **DOI:** 10.1088/1674-1056/22/6/068103

1. Introduction

In scanning probe microscopes (SPM), such as scanning tunneling microscopes (STM) and atomic force microscopes (AFM), piezoelectric scanners are used to provide the fine scanning and the positioning between the tip and sample.[1–3] Piezoelectric scanners typically have a simple structure, compact size and good thermal stability; many researchers still endeavor to develop new structures and study their scanning mechanisms to optimize and improve performance.[4–8] For an SPM with a Besocke-style scanner, the intrinsic vibrations induced by the probe-sample interface can limit the spatial resolution of the system.[4] For example, the atomic structure of the sample can excite vibrations in the range 500 Hz–1700 Hz when the scanning speeds are 1 Å/ms (1 Å = 0.1 nm) and higher.[5] The higher scanning speeds can induce vibrations at higher frequencies. If the excited resonance vibration is close to the intrinsic vibrations of the scanner, then the spatial resolution of the atomic structure is greatly reduced.

A Besocke-style scanner consists of a scanner head and a supporting ramp around the sample holder. In the scanner head, the scanner disk is supported by three outer piezoelectric positioning tubes. Each of these tubes has a non-rolling ball bearing affixed in its bottom end, and the three bearings rest on the ramp beside the sample. These three balls exhibit stick-slip behaviors, while the flexing tubes collectively move the scanning disk above the sample for coarse and fine positioning. A central cantilever holds the probe tip and is used for scanning the sample. By bending the three positioning tubes appropriately, the whole central cantilever along with the probe tip can be translated with respect to the sample in any given direction.

Generally, the probe-sample interface in a Besocke-style scanner induces stick-slip behavior of the balls on the supporting ramp. When the vibrations of the supporting ramp are induced by ambient noise, the stick-slip behavior becomes complex because the motion of a ball depends on the vibrations of the ramp as well as the probe-sample interface. Thus, the intrinsic vibrations of a Besocke-style scanner are complex and difficult to investigate. For designing and optimizing the scanners, it has become important to develop a clear insight into the physical mechanisms of the intrinsic vibrations.

The purpose of this paper is to present a theoretical model for investigating the intrinsic vibrations induced by the ramp's vibrational state and the microscopic contact. Meanwhile, we show the characteristics of the intrinsic vibrations induced by the stick-slip behavior, and provide a clear interpretation of the underlying physics.

2. Theoretic model

2.1. Lateral friction

For the harmonic vibration, the flexural resonance frequency of the piezo-tube on the ramp depends on the lateral force in the ball–ramp interactions. In experiments, the lateral force gives rise to the stick-slip behavior of the ball on the ramp.[9] At low vibration amplitudes, a ball sticks to the ramp and the lateral force can be described by a linear spring. In the

*Project supported by the National Basic Research Program of China (Grant No. 2012CB921504), the National Natural Science Foundation of China (Grant Nos. 11004099, 1174142, and 11274169), the Natural Science Foundation of Jiangsu Province of China (Grant No. BK2012721), the Fundamental Research Funds for the Central Universities (Grant No. 1126020435), and the Priority Academic Program Development of Jiangsu Higher Education Institutions.

†Corresponding author. E-mail: paslabw@nju.edu.cn

© 2013 Chinese Physical Society and IOP Publishing Ltd

sticking regime, the lateral friction can be given as

$$F_{\mathrm{Lat}} = K_{\mathrm{Lat}}[y(t) - u(t)], \tag{1}$$

$$K_{\mathrm{Lat}} = 8a_{\mathrm{c}}G^{*}, \tag{2}$$

where K_{Lat} is the lateral ball-ramp contact stiffness, $a_{\mathrm{c}} = \sqrt[3]{3R_{\mathrm{ball}}P_{\mathrm{Pre}}/4E^{*}}$, R_{ball} is the ball radius, P_{Pre} is the normal preload exerted on the ball-ramp interface, G^{*} is the equivalent shear modulus and E^{*} is the equivalent Young's modulus;[10] $y(t) = Y\cos(\omega t)$ and $u(t) = U\cos(\omega t + \varphi)$ denote the displacement of a ball and the ramp, respectively; ω is the angular frequency, t is time and φ is the initial phase; and Y and U are the vibration amplitudes of a ball and the ramp, respectively.

For a larger displacement in the ball–ramp contact, the ball begins to slip on the ramp when the lateral friction is larger than the threshold friction. The threshold friction F_{o} is equal to μP_{Pre}, and μ is the friction coefficient of the ball–ramp contact.[11] As a ball goes into the slipping motion, the lateral friction induced by the ball–ramp contact remains approximately constant. In this state, the force behavior can be modeled as a spring in series with a slider.[10]

For the lateral friction model, it is assumed that a constant normal preload is applied to the ball–ramp interface. When the ball–ramp interface is subjected to a cyclic motion, the stick-slip behavior shows a hysteresis loop behavior consisting of two symmetric sticking regions and two symmetric slipping regions, as shown in Fig. 1.[12]

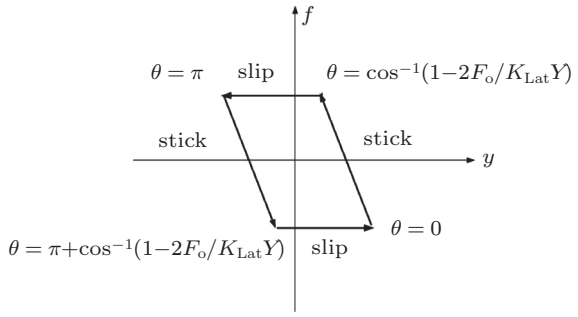


Fig. 1. The hysteresis loop of the lateral friction.

When the vibrations of the ramp are excited by ambient vibrations, a ball's motion relative to the vibrating ramp can be given as

$$z(t) = Y\cos\omega t - U\cos(\omega t + \varphi) = H\cos(\omega t - \theta_0), \tag{3}$$

where

$$H = \sqrt{Y^2 + U^2 - 2YU\cos\varphi}, \quad \theta_0 = \tan^{-1}\left(\frac{U\sin\varphi}{Y - U\cos\varphi}\right),$$
$$-\frac{\pi}{2} \le \theta_0 \le \frac{\pi}{2}; \quad \theta_0 = \pi + \tan^{-1}\left(\frac{U\sin\varphi}{Y - U\cos\varphi}\right),$$
$$\frac{\pi}{2} \le \theta_0 \le \frac{3}{2}\pi.$$

With knowledge of the hysteresis, the slipping-to-sticking transitions are predictable, always occurring at the instant when the relative motion reverses its direction ($\theta = \theta_0$ and $\theta = \theta_0 + \pi$). Thus, the lateral friction $f(t)$ in the interface between a ball and the vibrating ramp can be divided into four friction phases:

$$f(t) = \begin{cases} -K_{\mathrm{Lat}}H\cos(\omega t - \theta_0) + K_{\mathrm{Lat}}H - F_{\mathrm{o}}, & \theta_0 < \omega t \le \theta_0 + \cos^{-1}S; \\ F_{\mathrm{o}}, & \theta_0 + \cos^{-1}S < \omega t \le \pi + \theta_0; \\ -K_{\mathrm{Lat}}H\cos(\omega t - \theta_0) - K_{\mathrm{Lat}}H + F_{\mathrm{o}}, & \pi + \theta_0 < \omega t \le \pi + \theta_0 + \cos^{-1}S; \\ -F_{\mathrm{o}}, & \pi + \theta_0 + \cos^{-1}S < \omega t \le 2\pi + \theta_0; \end{cases} \tag{4}$$

where $S = 1 - 2F_{\mathrm{o}}/K_{\mathrm{Lat}}H$. When $1 < F_{\mathrm{o}}/K_{\mathrm{Lat}}H$, $S = -1$. By using the harmonic balance method, the nonlinear lateral friction $f(t)$ in Eq. (4) can be written as

$$f(t) \approx \left(A_1\cos(\omega t - \theta_0) + A_2\sin(\omega t - \theta_0)\right)/\pi, \tag{5}$$

where

$$A_1 = -(K_{\mathrm{Lat}}YS\sqrt{(1-S^2)} - 2K_{\mathrm{Lat}}Y\sqrt{(1-S^2)} + K_{\mathrm{Lat}}Y\arccos(S) + 4F_{\mathrm{o}}\sqrt{(1-S^2)}),$$

and

$$A_2 = K_{\mathrm{Lat}}Y + K_{\mathrm{Lat}}YS^2 - 2K_{\mathrm{Lat}}YS + 4SF_{\mathrm{o}}.$$

2.2. Model of flexural vibrations

Timoshenko beam theory is applied to investigate the flexural intrinsic vibrations with the lateral friction boundary conditions. Compared with the elastic stiffness, the piezoelectric stiffness can be ignored.[13] So the governing equations can be expressed as

$$\kappa GA\left(\frac{\partial w(z,t)}{\partial z} - \phi(z,t)\right) + EI\frac{\partial^2\phi(z,t)}{\partial z^2} - \rho I\frac{\partial^2\phi(z,t)}{\partial t^2} = 0, \tag{6}$$

$$\rho A\frac{\partial^2 w(z,t)}{\partial t^2} - \kappa GA\left(\frac{\partial^2 w(z,t)}{\partial z^2} - \frac{\partial\phi(z,t)}{\partial z}\right) = 0, \tag{7}$$

where the shear correction coefficient κ is determined by the outer and inner radii as well as Poisson's ratio of the tube; A is the cross-section's area; G is the shear modulus; E is the Young's modulus; I is the cross-section area moment of inertia; ρ is the density of the piezo-tube; and $w(z,t)$ and $\phi(z,t)$ are the transverse displacement and rotation angle, respectively, of the neutral axis of the piezo-tube during bending.

For the harmonic vibrations, defining $w(z,t) = W(z)\cos(\omega t)$, $\phi(z,t) = \psi(z)\cos(\omega t)$ and L is the length of the piezo-tube, $\xi = z/L$, $b^2 = \rho AL^4\omega^2/(EI)$, $r^2 = I/AL^2$, $s^2 = EI/\kappa AGL^2$. The solutions of Eqs. (6) and (7) can be given as[14]

$$\begin{aligned} W(\xi) &= C_1\cosh(b\alpha\xi) + C_2\sinh(b\alpha\xi) \\ &\quad + C_3\cos(b\beta\xi) + C_4\sin(b\beta\xi), \qquad (8) \\ \psi(\xi) &= k_1C_1\sinh(b\alpha\xi) + k_1C_2\cosh(b\alpha\xi) \\ &\quad + k_2C_3\sin(b\beta\xi) - k_2C_4\cos(b\beta\xi), \qquad (9) \end{aligned}$$

where C_1, C_2, C_3, C_4 are constants, and k_1, k_2, α, β are determined by r, s, b, L.

In a Besocke-style scanner, one end of the piezo-tube is soldered to the scanner disk and cannot bend at the soldered point, so the rotation angle should be zero. But the scanner disk can move laterally, which results in a shear force equal to the product of m_0 (the mass of the scanner disk and center cantilever with a probe) and acceleration of the scanner disk. Therefore, at $z = 0$ the corresponding boundary conditions are

$$\phi(z,t)|_{z=0} = 0, \qquad (10)$$

$$\kappa AG\left.\frac{\partial w(z,t)}{\partial z}\right|_{z=0} - \frac{m_0}{3}\left.\frac{\partial^2 w(z,t)}{\partial t^2}\right|_{z=0} = 0. \qquad (11)$$

The scanner disk is supported by three outer piezo-tubes, so each outer piezo-tube has a mass of one-third of m_0.

At the ball end of a piezo-tube, lateral friction is applied to the ball. At an arbitrary time, the vibrational behavior of the outer piezo-tube approximately satisfies the dynamic equilibrium of the shear force and moments. Therefore, at $z = L$ the boundary conditions can be given as

$$\left[\kappa AG\left(\frac{\partial w(z,t)}{\partial z} - \phi(z,t)\right) + m_1\frac{\partial^2 w(z,t)}{\partial t^2}\right]\Bigg|_{z=L} - f(t) = 0, \qquad (12)$$

$$\left[EI\frac{\partial\phi(z,t)}{\partial z} + J_1\frac{\partial^2\phi(z,t)}{\partial t^2}\right]\Bigg|_{z=L} - f(t)\cdot l = 0, \qquad (13)$$

where m_1 is the mass and J_1 is the inertia moment of the ball; and $l = R_{\rm ball} + (h - R_{\rm ball})\cos(\phi(L,t))$ is the length of the arm that incorporates the lateral friction moment. For vibration with a small rotational angle, it can be obtained as $l \approx R_{\rm ball} + (h - R_{\rm ball})$, in which h is the distance between the ramp surface and the piezo-tube's end at $z = L$, and $R_{\rm ball}$ is the radius of the ball bearing.

By substituting Eq. (5) into Eqs. (12) and (13), and multiplying by $\cos(\omega t - \theta_1)$ on both sides of the equations, one can integrate over one period $T = 2\pi/\omega$, and obtain

$$\left(\frac{1}{L}\frac{\partial Y(\xi)}{\partial\xi} - \psi(\xi) - \frac{1}{L}p_1b^2s^2Y(\xi)\right) - \frac{A_1}{\kappa\pi AG} = 0, \quad \xi = 1; \qquad (14)$$

$$\left(\frac{\partial\psi(\xi)}{\partial\xi} - q_1b^2\psi(\xi)\right) - \frac{A_1Ll}{\pi EI} = 0, \quad \xi = 1; \qquad (15)$$

where $p_1 = m_1/\rho AL$ and $q_1 = J_1/\rho AL^3$; and m_1 is the mass of the ball.

Substituting Eqs. (8) and (9) into Eqs. (10), (11), and (14), the following relations can be given

$$C_1 = B_1(C_4), \quad C_2 = B_2(C_4), \quad C_3 = B_3(C_4). \qquad (16)$$

The functions of B_1, B_2, and B_3 are determined by the geometrical and mechanical parameters of the scanner and the lateral friction. Thus, the general solutions of the $W(1)$ and $\psi(1)$ can be obtained. According to the geometrical relationship between $W(1)$, $\psi(1)$, and Y, for vibration with a small rotational angle one can get

$$Y \approx W(1) + (h - R_{\rm ball})\psi(1). \qquad (17)$$

If the vibration amplitude Y is measured in advance, C_4 can be derived from Eq. (17)

$$C_4 = D[Y]. \qquad (18)$$

Then, substituting Eqs. (16) and (18) into Eq. (15), the characteristic equation of flexural resonance frequencies for the scanner can be obtained.

3. Results and discussion

A scanner resting on three steel ball bearings on a steel ramp is investigated. The corresponding material and geometric parameters of the ball and the ramp are as follows: $E = 216$ GPa, $G = 84$ GPa, $\rho = 7800$ kg·m^{-3}, $v = 0.28$, $m_1 = 90$ mg, $R_{\rm ball} = 1.4$ mm, and $h = 2.26$ mm. In addition, the material and geometric parameters of the piezo-tube are as follows: $E = 61$ GPa, $G = 23$ GPa, $\rho = 7750$ kg·m^{-3}, $L = 10$ mm, the outer diameter of the piezo-tube $D = 3.2$ mm, the inner diameter of the piezo-tube $d = 2.2$ mm, and the mass of the scanner disk and center cantilever with a probe, $m_0 = 3$ g.[5] For the special case with a steel ball and a steel ramp, the lateral contact stiffness is 9.8×10^5 N/m.

3.1. Intrinsic vibrations of the scanner in the case of a steady ramp

A ball's motions on the ramp depend on the tribological characteristics of the ball–ramp interface, which has a close relationship to $F_{\rm o}/K_{\rm Lat}Y$. For example, $F_{\rm o}/K_{\rm Lat}Y = 0$, and $F_{\rm o}/K_{\rm Lat}Y \geq 1$ represent the pure slipping and pure sticking behaviors, respectively. In the pure slipping regime, $F_{\rm o}$ is much

less than $K_{\mathrm{Lat}}U$, i.e., $S \approx 1$. Here, the ball is not influenced by lateral friction. The critical case may emerge when there is superlubrication in the ball–ramp interface. When the elastic micro-deformation of the ball–ramp interaction is satisfied, the ball maintains a pure sticking behavior on the ramp, i.e., the threshold force F_{o} is larger than $K_{\mathrm{Lat}}U$. The lateral friction applied to the ball can be given as $f(t) = -K_{\mathrm{Lat}}Y\cos(\omega t)$. In this regime, the intrinsic vibrations depend on the lateral contact stiffness.[15]

As $0 < F_{\mathrm{o}}/K_{\mathrm{Lat}}Y < 1$, figure 2 shows the effects of F_{o} and Y on the intrinsic vibrations in the stick-slip regime. The scanner can be analyzed as a mass-spring system.[16] When the ramp is steady, the lateral friction applied on the ball can be taken as a force to inhibit the vibrations of the ball, in which the equivalent spring stiffness increases with the decrease in the integral friction in one vibration period for certain values of Y. Therefore, it is seen that with an increase in F_{o}, the resonance frequency decreases from 9795 Hz, which is the frequency in the slipping regime, to the low eigenfrequency of the scanner in the sticking regime, i.e., 4321 Hz. Here, the behavior of a ball on the ramp can be regarded as a transition from the pure slipping motion to the pure sticking state. On the other hand, F_{o}, corresponding to the falling edge of the frequencies, is influenced by the vibration amplitude Y. So the intrinsic vibrations of the scanner can be regulated by an external force or by an electric signal input to adjust Y.

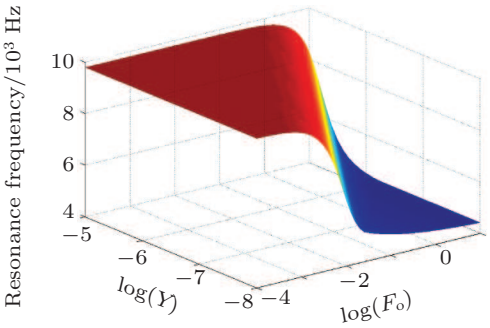


Fig. 2. (color online) Flexural vibration of a Besocke-style scanner on a steady ramp.

The fundamental flexural resonance frequencies of a Besocke-style scanner can be influenced by the motion state of the ball on the ramp, which is determined by $F_{\mathrm{o}}/K_{\mathrm{Lat}}Y$.[15] When $0 < F_{\mathrm{o}}/K_{\mathrm{Lat}}Y < 1$, a ball on the ramp maintains the stick-slip behavior. If $F_{\mathrm{o}}/K_{\mathrm{Lat}}Y$ tends to 0, the slipping motion dominates, and the ball's behavior can be described as a pure slipping motion on the ramp. If $F_{\mathrm{o}}/K_{\mathrm{Lat}}Y$ tends to 1, the sticking state dominates, and the ball's motion can be described as a pure sticking state on the ramp. If $F_{\mathrm{o}}/K_{\mathrm{Lat}}Y$ changes from 0 to 1, the ball's motion on the ramp can be regarded as a transition from the pure slipping motion to the pure sticking state.

3.2. Intrinsic vibrations of the scanner in the case of the vibrating ramp

Under this condition, the intrinsic vibrations are induced by the relative motion between the balls and the vibrating ramp. For a steady-state harmonic vibration, we can get $\varphi = 0$ and $U - Y < 0$ or $U - Y > 0$. If $\varphi = 0$ and $U - Y < 0$, the vibration amplitudes of the balls differ only in relation to the vibrating or steady ramp. The intrinsic vibrations of the scanner are similar to the case with the steady ramp, as shown in Fig. 2.

If $\varphi = 0$ and $U - Y > 0$, then the lateral friction applied to a ball has the same direction as the velocity of the ball. We changed $U - Y$ and F_{o} to investigate the characteristics of the intrinsic vibrations. The results are shown in Fig. 3. It can be seen that with an increase in F_{o}, the resonance frequencies increase from low values to a constant 4321 Hz.[7] Here, the intrinsic vibrations with the unexpected low resonance frequencies are excited, in which the frequencies are much lower than the lowest eigenfrequency, 4321 Hz, of the scanner in the sticking regime. The results can be confirmed by the measurements in Ref. [4]. These unexpected low resonance frequencies are attributed to the decrease in the equivalent spring stiffness with F_{o}. When $U - Y > 0$, the lateral friction applied to a ball excites the vibrations of the scanner, and the equivalent spring stiffness will decrease with the decrease of F_{o}, which for a small F_{o} means that a small driving friction arises in one vibration period for certain values of $U - Y$.

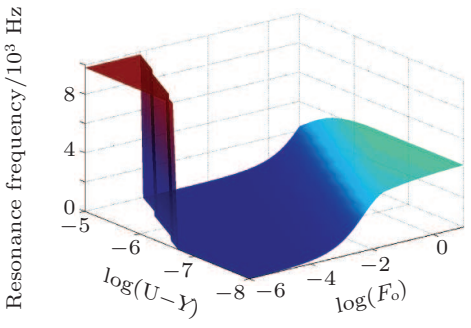


Fig. 3. (color online) Flexural vibration of a Besocke-style scanner on a vibrating ramp.

When F_{o} tends to zero, all scanners with either a vibrating or steady ramp have the same intrinsic vibration, 9795 Hz. In fact, the vibrations can be taken as the free vibrations of the scanner head, which are not influenced by the probe–sample interface as the lateral friction tends to zero. But the vibrational states are not stable, so they are susceptible to the tribological characteristics of the ball–ramp interface.

It should be pointed out that the periodical microscopic interface of the sample surface can excite micro-vibration in the probe tip, which moves with the positioning system. For typical sample surfaces, the frequency of such micro-vibrations is mainly in the range of 500 Hz–1700 Hz. In appli-

cations, an unexpected intrinsic vibration of the positioning system can easily be excited when the micro-vibration frequency is close to that of the system's intrinsic vibrations. Thus, the coupling vibration will severely reduce the spatial resolution of the scanner.

4. Conclusions

The intrinsic vibrations are distinctly influenced by the characteristics of the ball–ramp interface and the vibrational states of the ramp. For a steady ramp, the intrinsic vibrations essentially depend on the tribological characteristics of the interface, i.e., the ratio of the ball–ramp lateral friction threshold to the product of the ball–ramp lateral contact stiffness and the amplitude of the ball's vibration. For the vibrating ramp, unexpected vibration modes with lower frequencies can be excited. These unexpected vibration modes have a close relationship with the motions of the balls relative to the ramp. The theoretical model and results give clear insights into the intrinsic vibrations of Besocke-style scanners, and provide a way to regulate the excitation of the intrinsic vibrations by controlling the external force or the vibration amplitude of the balls on the ramp.

References

[1] Arnalds U B, Bjarnason E H, Jonsson K and Olafsson S 2006 *Appl. Sur. Sci.* **252** 5485
[2] Chen J M, Lin M M and Duan W S 2010 *Chin. Phys. B* **19** 026201
[3] Zhang H, Zhang S Y and Fan L 2012 *Chin. Phys. B* **21** 083302
[4] Behler S, Rose M K, Ogletree D F and Salmeron M 1997 *Rev. Sci. Instrum.* **68** 124
[5] Miwa J A, MacLeod J M, Moffat A and McLean A B 2003 *Ultramicroscopy* **98** 43
[6] Hua B C, Qian J Q, Wang X and Yao J E 2011 *Acta Phys. Sin.* **60** 040702 (in Chinese)
[7] Brukman M J and Carpick, R W 2006 *Rev. Sci. Instrum.* **77** 033706
[8] Chen J S, Ge Y and Zhang H 2012 *Chin. Phys. Lett.* **29** 010701
[9] Tambe N S and Bhushan B 2005 *J. Phys. D: Appl. Phys.* **38** 764
[10] Reinstadtler M, Rabe U, Goldade A, Bhushan B and Arnold W 2005 *Tribology International* **38** 533
[11] Huang P and Gong Z L 2011 *Acta Phys. Sin.* **60** 024601 (in Chinese)
[12] Yang B D, Chu M L and Meng C H 1998 *J. Sound Vib.* **210** 461
[13] Zhang H, Zhang S Y and Wang T H 2007 *Ultrasonics* **47** 82
[14] White M W D and Heppler G R 1995 *ASME J. Appl. Mech.* **62** 193
[15] Zhang H, Zhang S Y and Fan L 2012 *J. Phys. D: Appl. Phys.* **45** 035303
[16] Zhang H, Zhang S Y, Chen Z J and Fan L 2010 *IEEE Trans. Ultrason., Ferroelect., Freq. Control* **57** 1140